molecules

MDPI

Article

Electrochemical Enzyme Sensor Based on the Two-Dimensional Metal–Organic Layers Supported Horseradish Peroxidase

Yu Xiong [1], Chao Wang [1], YuanFei Wu [1], Chunhua Luo [2,*], Dongping Zhan [1] and Shizhen Wang [1,*]

[1] College of Chemistry and Chemical Engineering, Xiamen University, Xiamen 361005, China
[2] The First College of Clinical Medical Science, China Three Gorges University, Yichang 443003, China
* Correspondence: lchlgj2004@aliyun.com (C.L.); szwang@xmu.edu.cn (S.W.)

Abstract: Metal–organic frames (MOFs) have recently been used to support redox enzymes for highly sensitive and selective chemical sensors for small biomolecules such as oxygen (O_2), hydrogen peroxide (H_2O_2), etc. However, most MOFs are insulative and their three-dimensional (3D) porous structures hinder the electron transfer pathway between the current collector and the redox enzyme molecules. In order to facilitate electron transfer, here we adopt two-dimensional (2D) metal–organic layers (MOLs) to support the HRP molecules in the detection of H_2O_2. The correlation between the current response and the H_2O_2 concentration presents a linear range from 7.5 μM to 1500 μM with a detection limit of 0.87 μM (S/N = 3). The sensitivity, reproducibility, and stability of the enzyme sensor are promoted due to the facilitated electron transfer.

Keywords: electrochemical enzyme sensor; metal–organic layers; horseradish peroxidase; hydrogen peroxide

Citation: Xiong, Y.; Wang, C.; Wu, Y.; Luo, C.; Zhan, D.; Wang, S. Electrochemical Enzyme Sensor Based on the Two-Dimensional Metal–Organic Layers Supported Horseradish Peroxidase. *Molecules* **2022**, *27*, 8599. https://doi.org/10.3390/molecules27238599

Academic Editor: César Augusto Correia de Sequeira

Received: 8 October 2022
Accepted: 29 November 2022
Published: 6 December 2022

1. Introduction

HRP-based electrochemical biosensors are of great importance for the rapid, accurate, and reliable detection of H_2O_2 in medical diagnosis as well as in food, pharmacy, and environment analysis [1–3]. Because the redox center of HRP is embedded in the hydrophobic amino acid residues, the electron transfer pathway between the HRP and the electrode is crucial for the high level of activity and selectivity of the biosensor. Chemically modified electrodes (CMEs) were proposed to solve this problem by optimizing the molecular orientations of HRP on CMEs by the surface charge or nanostructures as well as by facilitating the conductive network of electron transfer [4,5]. For example, the protonated amino groups are usually grafted on the CMEs surface to provide the electrostatic microenvironment for the molecular orientation of HRP since it is overall negatively charged [6]; and the metal nanoparticles [7], carbon nanotubes [8], and graphene [9,10] were adopted as current collectors to form the electron transfer network.

Three-dimensional porous materials have been widely used as enzyme immobilization carriers due to their tunable structure, high specific surface area, and high biocompatibility, including kaolin [11], zeolites [12], MOFs [13], etc. MOFs are widely used for sensors due to their large surface area, adjustable pore size, and functional sites. Li et al. highlighted the most recent progress in MOF for the sensing and switching materials in the detection of gases and volatile organic compounds [14]. Koo et al. reviewed the current application of pure MOFs, MOF membranes, and MOF derivatives as chemiresistors, as well as the future development of MOFs [15]. Fan et al. reported a $[(ZIF\text{-}8@HRP/GO)/(GO\text{-}PEI)]_4/ITO$ biosensor, and the current–concentration response was linear in the range of [20, 6000] μM with a detection limit of 3.4 μM (S/N = 3) [16]. Employing ZIF-67(Co), Liu et al. reported a linear current–concentration response region of [1.86, 1050] μM and a sensitivity of 315 $\mu A \cdot mM^{-1} \cdot cm^{-2}$ [17]. With a NH_2-MIL-53(Fe)/HRP/MWNTs/GCE, Jiang et al. found two linear current–concentration response ranges of [0.1, 1] μM and [1, 600] μM with a

detection limit of 0.028 μM [2]. However, these materials are generally of poor conductivity for electron transfer and, moreover, their surface stacking limits the mass transfer of the substrate, e.g., H_2O_2 for HRP [18].

A two-dimensional metal–organic framework has an ultrathin layer structure, which increases the exposed active sites, reduces the resistance and, ultimately, improves its catalytic performance. It is widely used in water splitting reactions, the electro-oxidation of organic molecules, etc. [19]. Here, we adopted a novel ordered 2D material, termed as metal–organic layers (MOLs), NH_2-Hf-BTB-MOL, as the supporter of HRP molecules to construct the electrochemical H_2O_2 sensor. The results show that the 2D MOL-based sensor cannot only facilitate the electron transfer by shortening the transfer distance, but also improve the effective loading amount of HRP, demonstrating the prospective applications of 2D MOLs in electrochemical enzyme sensors.

2. Results and Discussions

The voltammetric behaviors of the CMEs, including the MWNTs/CC (Curve a), HRP/MWNTs/CC (Curve b), NH_2-Hf-BTB-MOL/MWNTs/CC (Curve c), and HRP/NH_2-Hf-BTB-MOL/MWNTs/CC (Curve d) electrodes, are shown in Figure 1A. Comparing Curve a and Curve c, the charging/discharging currents of the electric double layer were almost doubled, indicating that the electric double-layer (EDL) capacitance of the NH_2-Hf-BTB-MOL/MWNTs/CC electrode was larger than that of the MWNTs/CC electrodes. Meanwhile, a pair of redox peaks at −0.38 V were observed in both Curve b and Curve d. It was observed that the Faraday current response on the HRP/NH_2-Hf-BTB-MOL/MWNTs/CC electrode was enhanced much higher than that on HRP/MWNTs/CC electrode. The ratio of Faraday current caused by the redox reaction of HRP over the charging/discharging current of EDL was also improved on the HRP/NH_2-Hf-BTB-MOL/MWNTs/CC electrode. The results show the facilitated charge transfer between the MWNT/CC network and the HRP molecules immobilized on the 2D MOL through the static interaction between the protonated amino groups and HRP molecules.

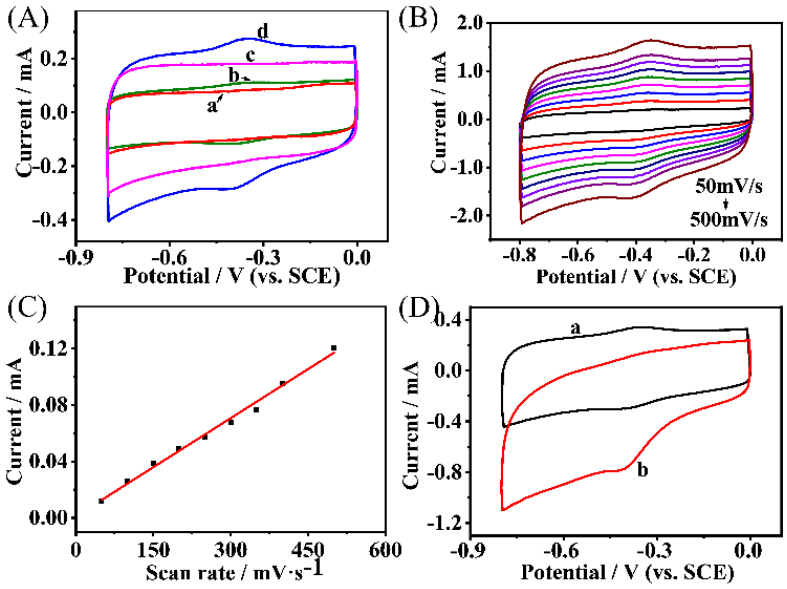

Figure 1. (**A**) Cyclic voltammograms obtained on the modified electrodes in 0.1 M PBS (pH = 7.0) at a scan rate of 100 mV/s: (a) MWNTs/CC; (b) HRP/MWNTs/CC; (c) NH_2−Hf−BTB−MOL/MWNTs/CC; and (d) HRP/NH_2−Hf−BTB−MOL/MWNTs/CC. (**B**) Cyclic voltammograms of the HRP/NH_2−Hf−BTB−MOL/MWNTs/CC electrode in 0.1 M PBS (pH = 7.0) at different scan rates. (**C**) The linear relationship between the peak current and the scan rate. (**D**) Cyclic voltammograms of the HRP/NH_2−Hf−BTB−MOL/MWNTs/CC electrode in 0.1 M PBS (pH = 7.0) with a scan rate of 100 mV/s: (a) in the absence of H_2O_2; and (b) in the presence of 1.5 mM H_2O_2.

Figure 1B shows the cyclic voltammograms with the different scan rates obtained on the HRP/NH_2-Hf-BTB-MOL/MWNTs/CC electrode. Since the HRP molecules were immobilized on the 2D MOL, the typical voltammetric characteristics of redox adsorption species are presented. The peak potential hardly moved with the scanning rate, and the peak current was found in harmonious proportion to the scan rate (Figure 1C), indicating that the kinetic rate of the HRP redox reaction was pretty reversible. Thus, the effective loading of HRP can be obtained by the following equation [20]:

$$i_p = \frac{n^2F^2A\Gamma v}{4RT} \quad (1)$$

where i_p is the peak current, n is electron transfer number (n = 1), F is the Faraday constant (96,485 C·mol^{-1}), R is the gas constant (8.314 J·K^{-1}·mol^{-1}), and T is the experimental temperature (298.15 K), A is an apparent electrode area, Γ is the apparent surface concentration, and v is the scan rate (V·s^{-1}). From Equation (1), Γ was calculated as 3.88×10^{-10} mol·cm^{-2} on the HRP/NH_2-Hf-BTB-MOL/MWNTs/CC electrode, which was 3.3-fold higher than that on HRP/MWNTs/CC electrode (1.17×10^{-10} mol·cm^{-2}), and 10-fold higher than that in previous reports [21–23]. The quantitative results demonstrated that the planar structure of the 2D MOL can improve the effective loading amount of HRP molecules. The voltammetric behavior of the HRP electrocatalytic reduction of H_2O_2 obtained on the HRP/NH_2-Hf-BTB-MOL/MWNTs/CC electrode is shown in Figure 1D.

To further elucidate the effect of the 2D MOL on the HRP redox reaction, EIS experiments were performed and the results are shown in Figure 2. In the presence of 2D MOL, the charge transfer resistance becomes smaller, indicating that the kinetic rate of electron transfer was improved. Since the 2D MOL has a nanometer thickness and is homogeneously distributed on the MWNTs network, compared with the 3D materials, the tunnel distance of electron transfer between the MWNTs network and the HRP molecules was shortened, and the Faraday current was enhanced in cyclic voltammetry (Figure 1A). However, the EDL capacitance becomes higher in the presence of the 2D MOL in cyclic voltammetry. In general, if the specific capacitance of the electrode material is known, the EDL capacitance can be adopted to estimate the "real" surface or interface area, which is usually higher than the "geometric" area and, in some case, is considered as the active electrode area [24]. Nevertheless, an ultrathin 2D material or even a molecular monolayer (e.g., thiol on gold) could not dramatically change the electrode surface area. Because of the dielectric properties (ε: dielectric constant) of the modified material, the EDL capacity of CMEs usually becomes larger than the bare electrodes or the MWNTs modified electrodes ($C = \varepsilon S/d$, here S is the area and d is the thickness). Thus, the real area could not be obtained simply by the EDL capacitance for most CMEs without knowing the dielectric constant and specific capacitance of the modified materials. Fortunately, because the electrochemical sensors work under the steady state, the capacitance affects the response time, but not the detection accuracy. The EIS experiment results (Figure 2) showed that the apparent charge transfer resistance became smaller in the presence of 2D MOL (102 Ω) compared with that in the absence of 2D MOL (170 Ω); meanwhile, the apparent EDL capacitance was obtained as 46.6 μF in the presence of 2D MOL compared with that in the absence of 2D MOL (18.9 μF). The results are in harmonious accordance with those of cyclic voltammetry. It can be concluded that the 2D MOL, as a modified electrode material, cannot only improve the effective loading amount of HRP molecules, but also facilitate electron transfer between the HRP molecules and MWNT/CC conductive network, which predicts an excellent sensing performance, as subsequently shown in Table 1.

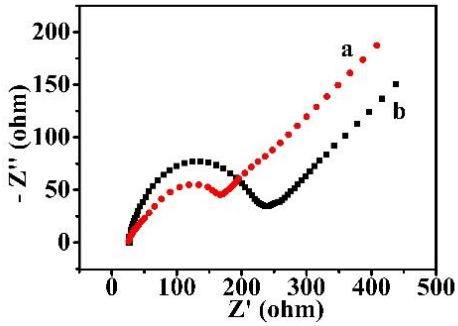

Figure 2. The EIS spectra of (a) HRP/NH_2-Hf-BTB-MOL/MWNTs/CC; and (b) HRP/MWNTs/CC electrodes in the 0.1 M PBS solution.

Figure 3A shows the effect of pH on the performance of the HRP/NH_2-Hf-BTB-MOL/MWNTs/CC electrode in the absence of H_2O_2. The peak potential of HRP redox reduction shifted negatively with the increased pH value with a slope of -53.26 mV·pH^{-1}, indicating it was a proton-coupled single electron transfer reaction [25]. Considering the biological environment and the Faraday current response, a pH value of 7.0 was chosen to test the sensing performance. To optimize the effective loading amount of HRP on the 2D MOL, a different mass ratio was tried during the pre-loading process when preparing the CME by fixing the concentration of NH_2-Hf-BTB-MOL at 0.25 mg/mL and the volume at 1 mL. From Figure 3B, it can be seen that the Faraday current response achieves its maximum when the mass ratio of MOF over HRP is 1:4. When the amount of HRP is lower, the adsorption of HRP is not saturated. However, when the amount of HRP is higher, the overlapped HRP can hinder the effective usage of HRP.

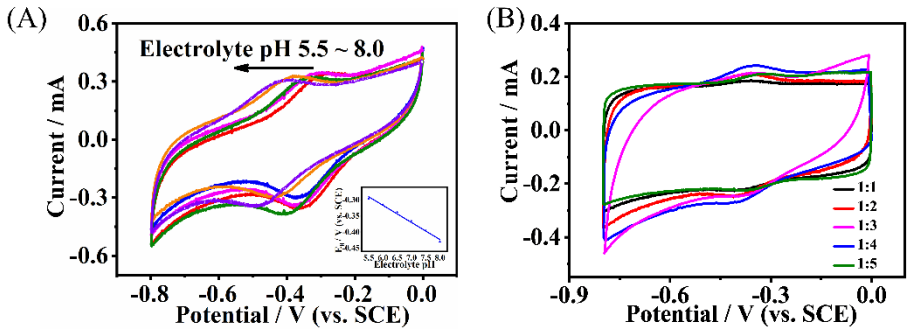

Figure 3. (**A**) Cyclic votammograms obtained on the HRP/NH_2-Hf$-$BTB$-$MOL/MWNTs/CC electrode in 0.1 M PBS at different pH values: 5.5, 6.0, 6.5, 7.0, 7.5, 8.0. Inset: linear relationships of E_θ with buffer pH. (**B**) Cyclic votammograms obtained on the HRP/NH_2-Hf$-$BTB$-$MOL/MWNTs/CC electrode with different MOF: HRP ratio in 0.1 M PBS (pH = 7.0). The scan rate is 100 mV/s.

Successive-sample-injection chronoamperometry was carried out to evaluate the sensing performance of the HRP/NH_2-Hf-BTB-MOL/MWNTs/CC electrode. The applied potential was fixed at -0.4 V and the steady-state Faraday current responses with the injected H_2O_2 concentration were recorded, as shown in Figure 4A. The linear relationship between the current response and the H_2O_2 concentration ranged from 7.5 μM to 1.5 mM (Figure 4B). Additionally, the sensitivity and detection limit were obtained as 282.4 μA·mM^{-1} ·cm^{-2} and 0.87 μM (S/N = 3). The affinity of H_2O_2 on the HRP/NH_2-Hf-BTB-MOL/MWNTs/CC electrode was also evaluated by the Lineweaver–Burk equation [26]:

$$\frac{1}{I_{ss}} = \frac{1}{I_{max}} + \frac{K_m{}^{app}}{I_{max}C} \quad (2)$$

where $K_m{}^{app}$ is the Michaelis–Menten constant, I_{ss} is the steady-state current after H_2O_2 injection, C is the concentration of H_2O_2, and I_{max} is the limiting enzyme-catalytic current

when H_2O_2 is saturated. The K_m^{app} was obtained as 0.22 mM from the linear relationship between $1/I_{ss}$ and $1/C$ (as the insert in Figure 4B), indicating the good affinity of H_2O_2 on the HRP/NH_2-Hf-BTB-MOL/MWNTs/CC electrode. Compared with previous reports, this 2D-MOL supported enzyme biosensor presents high sensitivity and high affinity, as listed in Table 1.

Table 1. Parameters of the reportedly modified HRP electrodes.

HRP Electrodes	Sensitivity ($\mu A \cdot mM^{-1} \cdot cm^{-2}$)	Linear Range (μM)	LOD (μM)	K_m (μM)	Reference
HRP/GO-Co_3O_4-Nafion/GCE	18.7 ± 0.5	1000–30,000	2000	—	[27]
PEDOT/PB/PPyBA/HRP	1.15	100–700	30	-	[28]
HRP/chitosan-$NiFe_2O_4$/GCE	0.314	300–1200	14	1400	[29]
HRP/TBA−COOH−IL/MWCNT/GCE	160.6	20–4300	6	—	[30]
[(ZIF-8@HRP/GO)/(GO-PEI)]$_4$/ITO	—	20–6000	3.4	9250	[16]
HRP/SiO_2/BSA/Au	—	8–3720	2.0	2300	[31]
HRP/GO/GCE	120	2–500	1.6	—	[32]
BPT/AuNPs/graphene/HRP/Au	—	5–2500	1.5	—	[33]
HRP/PDA-MNPs/(l-Arg/Tb)/GCE	—	0.5–30	0.23	—	[34]
NH_2-MIL-53(Fe)/HRP/MWNTs/GCE	—	0.1–1, 1–600	0.028	—	[2]
HRP/MWNTs/CC	185.2	50–600	5.8	330	This work
HRP/NH_2-Hf-BTB-MOL/MWNTs/CC	282.4	7.5–1500	0.87	220	This work

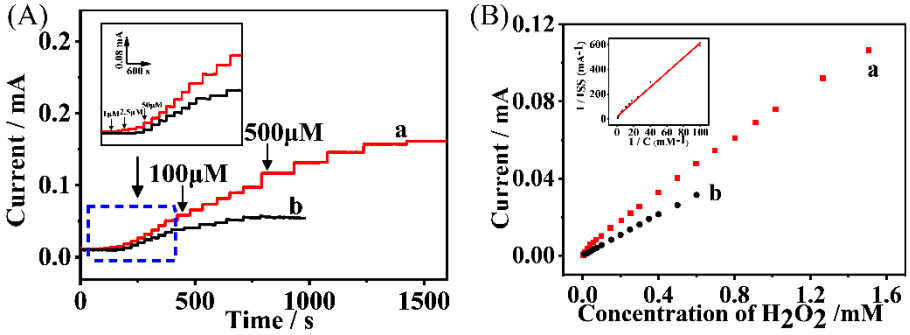

Figure 4. (**A**) The chronoamperometric curves recorded at −0.4 V with the successive injection of H_2O_2: (a) the HRP/NH_2−Hf−BTB−MOL/MWNTs/CC electrode; and (b) the HRP/MWNTs/CC electrode—the insert is the current response at low concentrations of H_2O_2. (**B**) The linear relationship between the Faraday current response and the concentration of H_2O_2 and the insert is the reciprocal relationship between the Faraday current response and the concentration of H_2O_2.

The interference performance caused by the electroactive substrates in the human body such as glucose, uric acid, ascorbic acid, lysine, dopamine, etc., were investigated [17,35]. The concentration of each interference substance used was 2 mM, i.e., 2-fold of that of H_2O_2 (1 mM) in the experiment. As shown in Figure 5A, these substrates did not affect the electrochemical detection of H_2O_2 because of the specific reduction of HRP to H_2O_2. Moreover, five groups of parallel experiments were performed in the presence of 0.5 mM H_2O_2 and the relative standard deviation of the Faraday current was 1.36%, indicating the good reproducibility of the preparation protocols of the HRP/NH_2-Hf-BTB-MOL/MWNTs/CC electrode. Moreover, after 50 cycles, the Faraday current was kept at 91.49% of the original (Figure 5B), which indicated the good stability of this biosensor. All the above results show that the 2D MOL materials have significant potential in the applications of electrochemical biosensors.

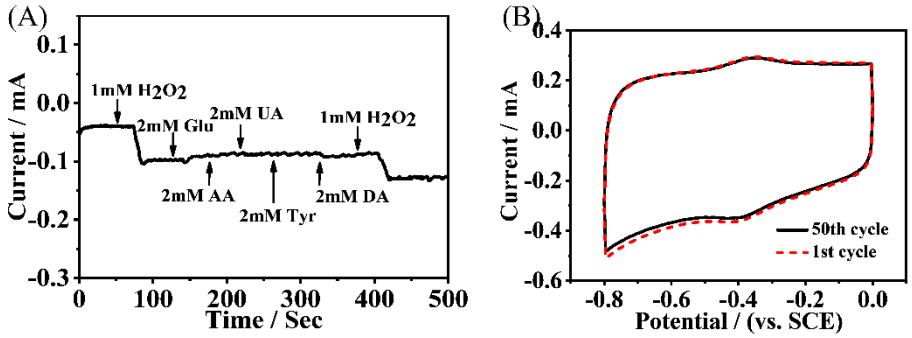

Figure 5. (**A**) HRP/NH_2-Hf-BTB-MOL/MWNTs/CC amperometric response to 2 mM different interfering substances (−0.4 V vs. SCE); and (**B**) Stability of HRP/NH_2-Hf-BTB-MOL/MWNTs/CC in 0.1 M PBS (pH = 7.0) containing 0.5 mM H_2O_2.

3. Materials and Methods

3.1. Chemicals and Materials

Carbon cloth (CC) was purchased from Carbon Energy Technology Co., Ltd. (Taiwan, China). Multi-walled carbon nanotubes (MWNTs) was purchased from Nanjing XFNANO Materials Technology Co., Ltd. (Nanjing, China). Nafion (5 wt%) was purchased from Guangzhou Lige Technology Co., Ltd. (Guangzhou, China). Ready-to-use PBS powder was purchased from Shanghai Sangon Biotech Co., Ltd. (Shanghai, China). Horseradish peroxidase (HRP), uric acid (UA), ascorbic acid (AA), glucose (Glu), dopamine (DA), and tyrosine (Tyr) were obtained from Aladdin Biochemical Technology Co., Ltd. (Shanghai, China). Aqueous solutions used in the experiments were prepared with deionized water (18.2 MΩ·cm, Milli-Q, Millipore Co.). Nitrogen gas (N_2, 99.999%) was purchased from Linde Gas Co.

3.2. The Fabrication of HRP/NH_2-Hf-BTB-MOL Modified Electrodes

The 2D MOL was a gift from Dr. Huihui Hu who is with Prof. Cheng Wang' group at Xiamen University [36]. NH_2-Hf-BTB-MOL was prepared by grafting an amino-terminated group by stirring 30 mL Hf-BTB-MOL (60 mM based on Hf in H_2O) and 50 mg ethanolamine phosphate at 60 °C overnight. HRP molecules were pre-loaded on the newly prepared NH_2-Hf-BTB-MOL by ultrasonic dispersion (Ultrasonic cleaner, KQ5200DE, Kunshan Ultrasonic Instrument Co., Ltd., Kunshan, China) of their mixture with different mass ratios in a 400 μL PBS buffer (0.1 M, pH = 7.0), and a subsequent constant-temperature oscillation (constant temperature water bath oscillator, SHA-C, Changzhou Xiangtian, Changzhou, China) for 1 h at 4 °C.

Carbon cloth (CC) was cut into pieces of 1 cm × 1 cm, alternately washed with acetone, ethanol, and water for 5 min, and dried on a heating plate. Then, 1 mg/mL MWNTs was dispersed ultrasonically in ethanol solution for 30 min. Subsequently, a 20 μL MWNTs suspension was dropped onto the CC piece to form a MWNTs/CC current collection network. After that, 20 μL HRP/NH_2-Hf-BTB-MOL suspension was drop-coated on the MWNTs/CC and dried at room temperature. Finally, 20 μL Nafion solution (5 wt%) was dropped to solidify the coatings. The prepared HRP/NH_2-Hf-BTB-MOL/MWNTs/CC electrode was stored in a refrigerator at 4 °C for use. For comparison, the MWNTs/CC, HRP/MWNTs/CC, and NH_2-Hf-BTB-MOL/MWNTs/CC electrodes were also prepared with the same protocols as schemed in Figure 6A. The SEM images of the MWNTs/CC and the NH_2-Hf-BTB-MOL/MWNTs/CC-modified electrodes are shown in Figure 6B,C.

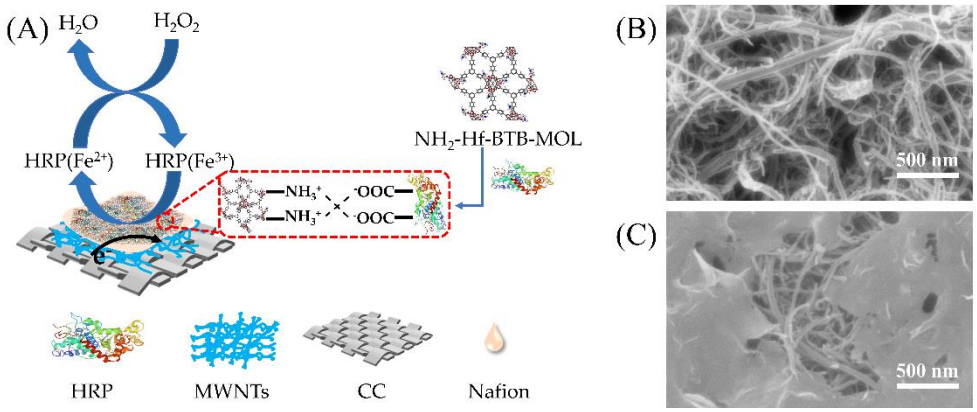

Figure 6. (**A**) Schematic diagram for H_2O_2 detection on the HRP/NH_2−Hf−BTB−MOL/MWNTs/CC biosensor; and (**B**,**C**) the SEM images of the MWNTs/CC and the NH_2−Hf−BTB−MOL/MWNTs/CC modified electrodes, respectively.

3.3. Electrochemical Measurements

Electrochemical experiments were performed with a CHI 850D electrochemical workstation (Shanghai Chenhua Co., Shanghai, China). Electrochemical impedance spectroscopy (EIS) experiments were performed with Autolab electrochemical workstation (Ω Metrohm Co., Herisau, Switzerland). A three-electrode system was adopted, where a saturated calomel electrode (SCE) and a platinum (Pt) wire electrode served as the reference electrode and counter electrode, respectively. The solution was bubbled gently by high-purity N_2 to degas oxygen before experiment.

4. Conclusions

Employing a 2D NH_2-Hf-BTB-MOL material as the support for HRP, we developed an electrochemical biosensor for the rapid, reliable, and precise detection of H_2O_2. Both the direct redox behaviors of HRP molecules and the electrocatalytic reduction of H_2O_2 were observed on the HRP/NH_2-Hf-BTB-MOL/MWNTs/CC electrode. By optimizing the pH value and effective loading amount of HRP, we found that the electrochemical enzyme sensor has excellent sensitivity, selectivity, affinity, and stability to H_2O_2. All the results indicate that the 2D MOLs have significant potential in the applications of electrochemical enzyme sensors because the ultrathin 2D MOLs cannot only facilitate the electron transfer, but also improve the effective loading amount of the enzyme molecules.

Author Contributions: Conceptualization, D.Z. and S.W.; Methodology, C.W., Y.W., C.L. and S.W.; Formal analysis, Y.X.; Data curation, Y.X.; Writing—original draft, Y.X.; Writing—review & editing, S.W.; Project administration, D.Z.; Funding acquisition, S.W. All authors have read and agreed to the published version of the manuscript.

Funding: This research was funded by the National Natural Science Foundation of China (No. 22078273, 21776233).

Institutional Review Board Statement: Not applicable.

Informed Consent Statement: Not applicable.

Data Availability Statement: The authors confirm that the data supporting the findings of this study are available within the article and its supplementary materials.

Conflicts of Interest: The authors declare no conflict of interest.

Sample Availability: Samples of the compounds are available from the authors upon reasonable request.

References

1. Wang, P.; Li, S.; Kan, J. A hydrogen peroxide biosensor based on polyaniline/FTO. *Sens. Actuators B-Chem.* **2009**, *137*, 662–668. [CrossRef]
2. Jiang, T.; Sun, X.; Wei, L.; Li, M. Determination of hydrogen peroxide released from cancer cells by a Fe-Organic framework/horseradish peroxidase-modified electrode. *Anal. Chim. Acta* **2020**, *1135*, 132–141. [CrossRef] [PubMed]
3. Kang, X.B.; Pang, G.C.; Liang, X.Y.; Wang, M.; Liu, J.; Zhu, W.M. Study on a hydrogen peroxide biosensor based on horseradish peroxidase/GNPs-thionine/chitosan. *Electrochim. Acta* **2012**, *62*, 327–334. [CrossRef]
4. Nikolaev, K.G.; Ermakov, S.S.; Ermolenko, Y.E.; Navolotskaya, D.V.; Offenhaeusser, A.; Mourzina, Y.G. Horseradish Peroxidase-Based Biosensors with Different Nanotransducers for the Determination of Hydrogen Peroxide. *J. Anal. Chem.* **2021**, *76*, 510–517. [CrossRef]
5. Thenmozhi, K.; Narayanan, S.S. Horseradish peroxidase and toluidine blue covalently immobilized leak-free sol-gel composite biosensor for hydrogen peroxide. *Mater. Sci. Eng. C-Mater. Biol. Appl.* **2017**, *70*, 223–230. [CrossRef] [PubMed]
6. Shimada, H.; Noguchi, S.; Yamamoto, M.; Nishiyama, K.; Kitamura, Y.; Ihara, T. Electrochemical Sensing of Neurotoxic Agents Based on Their Electron Transfer Promotion Effect on an Au Electrode. *Anal. Chem.* **2017**, *89*, 5743–5748. [CrossRef] [PubMed]
7. Chen, S.; Xie, Y.; Guo, X.; Sun, D. Self-supporting electrochemical sensors for monitoring of cell-released H_2O_2 based on metal nanoparticle/MOF nanozymes. *Microchem. J.* **2022**, *181*, 107715. [CrossRef]
8. Huang, J.D.; Yang, Y.; Shi, H.B.; Song, Z.; Zhao, Z.X.; Anzai, J.; Osa, T.; Chen, Q. Multi-walled carbon nanotubes-based glucose biosensor prepared by a layer-by-layer technique. *Mater. Sci. Eng. C-Biomim. Supramol. Syst.* **2006**, *26*, 113–117. [CrossRef]
9. Kim, T.-H.; Lee, D.; Choi, J.-W. Live cell biosensing platforms using graphene-based hybrid nanomaterials. *Biosens. Bioelectron.* **2017**, *94*, 485–499. [CrossRef]
10. Xu, J.; Wang, Y.; Hu, S. Nanocomposites of graphene and graphene oxides: Synthesis, molecular functionalization and application in electrochemical sensors and biosensors. A review. *Microchim. Acta* **2017**, *184*, 1–44. [CrossRef]
11. Torvinen, K.; Pettersson, F.; Lahtinen, P.; Arstila, K.; Kumar, V.; Österbacka, R.; Toivakka, M.; Saarinen, J.J. Nanoporous kaolin—Cellulose nanofibril composites for printed electronics. *Flex. Print. Electron.* **2017**, *2*, 024004. [CrossRef]
12. Soldatkin, O.O.; Kucherenko, I.S.; Shelyakina, M.K.; Soy, E.; Kirdeciler, K.; Ozturk, S.; Jaffrezic-Renault, N.; Akata, B.; Dzyadevych, S.V.; Soldatkin, A.P. Application of Different Zeolites for Improvement of the Characteristics of a pH-FET Biosensor Based on Immobilized Urease. *Electroanalysis* **2013**, *25*, 468–474. [CrossRef]
13. Feng, Y.; Xu, Y.; Liu, S.; Wu, D.; Su, Z.; Chen, G.; Liu, J.; Li, G. Recent advances in enzyme immobilization based on novel porous framework materials and its applications in biosensing. *Coord. Chem. Rev.* **2022**, *459*, 214414. [CrossRef]
14. Li, H.Y.; Zhao, S.N.; Zang, S.Q.; Li, J. Functional metal-organic frameworks as effective sensors of gases and volatile compounds. *Chem. Soc. Rev.* **2020**, *49*, 6364–6401. [CrossRef] [PubMed]
15. Koo, W.-T.; Jang, J.-S.; Kim, I.-D. Metal-Organic Frameworks for Chemiresistive Sensors. *Chem* **2019**, *5*, 1938–1963. [CrossRef]
16. Fan, Z.; Wang, J.; Nie, Y.; Ren, L.; Liu, B.; Liu, G. Metal-Organic Frameworks/Graphene Oxide Composite: A New Enzymatic Immobilization Carrier for Hydrogen Peroxide Biosensors. *J. Electrochem. Soc.* **2016**, *163*, B32–B37. [CrossRef]
17. Liu, X.; Chen, W.; Lian, M.; Chen, X.; Lu, Y.; Yang, W. Enzyme immobilization on ZIF-67/MWCNT composite engenders high sensitivity electrochemical sensing. *J. Electroanal. Chem.* **2019**, *833*, 505–511. [CrossRef]
18. Wang, Z.; Huang, J.; Mao, J.; Guo, Q.; Chen, Z.; Lai, Y. Metal-organic frameworks and their derivatives with graphene composites: Preparation and applications in electrocatalysis and photocatalysis. *J. Mater. Chem. A* **2020**, *8*, 2934–2961. [CrossRef]
19. Soni, I.; Kumar, P.; Kudur Jayaprakash, G. Recent advancements in the synthesis and electrocatalytic activity of two-dimensional metal–organic framework with bimetallic nodes for energy-related applications. *Coord. Chem. Rev.* **2022**, *472*, 214782. [CrossRef]
20. Yang, S.; Ding, S.; Li, L.; Ding, S.; Cao, Q.; Yang, J.; Xu, W.; Chen, A. One-Step Preparation of Direct Electrochemistry HRP Biosensor via Electrodeposition. *J. Electrochem. Soc.* **2017**, *164*, B710–B714. [CrossRef]
21. Chen, X.; Peng, X.; Kong, J.; Deng, J. Facilitated electron transfer from an electrode to horseradish peroxidase in a biomembrane-like surfactant film. *J. Electroanal. Chem.* **2000**, *480*, 26–33. [CrossRef]
22. Liu, X.; Huang, Y.; Shang, L.; Wang, X.; Xiao, H.; Li, G. Electron transfer reactivity and the catalytic activity of horseradish peroxidase incorporated in dipalmitoylphosphatidic acid films. *Bioelectrochemistry* **2006**, *68*, 98–104. [CrossRef] [PubMed]
23. Komori, K.; Terse-Thakoor, T.; Mulchandani, A. Electrochemical properties of seamless three-dimensional carbon nanotubes-grown graphene modified with horseradish peroxidase. *Bioelectrochemistry* **2016**, *111*, 57–61. [CrossRef] [PubMed]
24. Voiry, D.; Chhowalla, M.; Gogotsi, Y.; Kotov, N.A.; Li, Y.; Penner, R.M.; Schaak, R.E.; Weiss, P.S. Best Practices for Reporting Electrocatalytic Performance of Nanomaterials. *ACS Nano* **2018**, *12*, 9635–9638. [CrossRef]
25. Zheng, W.; Chen, W.; Weng, W.; Liu, L.; Li, G.; Wang, J.; Sun, W. Direct electron transfer of horseradish peroxidase at Co_3O_4-graphene nanocomposite modified electrode and electrocatalysis. *J. Iran. Chem. Soc.* **2017**, *14*, 925–932. [CrossRef]
26. Kafi, A.K.M.; Naqshabandi, M.; Yusoff, M.M.; Crossley, M.J. Improved peroxide biosensor based on Horseradish Peroxidase/Carbon Nanotube on a thiol-modified gold electrode. *Enzym. Microb. Technol.* **2018**, *113*, 67–74. [CrossRef]
27. Asif, S.A.B.; Khan, S.B.; Asiri, A.M. Electrochemical sensor for H_2O_2 using a glassy carbon electrode modified with a nanocomposite consisting of graphene oxide, cobalt(III) oxide, horseradish peroxidase and nafion. *Microchim. Acta* **2016**, *183*, 3043–3052. [CrossRef]

28. Ernst, A.; Makowski, O.; Kowalewska, B.; Miecznikowski, K.; Kulesza, P.J. Hybrid bioelectrocatalyst for hydrogen peroxide reduction: Immobilization of enzyme within organic-inorganic film of structured Prussian Blue and PEDOT. *Bioelectrochemistry* **2007**, *71*, 23–28. [CrossRef]
29. Yalciner, F.; Cevik, E.; Senel, M.; Baykal, A. Development of an Amperometric Hydrogen Peroxide Biosensor based on the Immobilization of Horseradish Peroxidase onto Nickel Ferrite Nanoparticle-Chitosan Composite. *Nano-Micro Lett.* **2011**, *3*, 91–98. [CrossRef]
30. Murphy, M.; Theyagarajan, K.; Thenmozhi, K.; Senthilkumar, S. Quaternary Ammonium Based Carboxyl Functionalized Ionic Liquid for Covalent Immobilization of Horseradish Peroxidase and Development of Electrochemical Hydrogen Peroxide Biosensor. *Electroanalysis* **2020**, *32*, 2422–2430. [CrossRef]
31. Yuan, S.; Yuan, R.; Chai, Y.; Zhuo, Y.; Yang, X.; Yuan, Y. Enzyme biosensor based on the immobilization of HRP on SiO_2/BSA/Au composite nanoparticles. *Appl. Biochem. Biotechnol.* **2010**, *162*, 2189–2196. [CrossRef] [PubMed]
32. Wang, Y.; Zhao, K.; Zhang, Z.; Jia, H.; Chen, J.; Fu, C. Simple Approach to Fabricate a Highly Sensitive H2O2 Biosensor by One-Step of Graphene Oxide and Horseradish Peroxidase Co-immobilized Glassy Carbon Electrode. *Int. J. Electrochem. Sci.* **2018**, *13*, 2921–2933. [CrossRef]
33. Wang, T.; Zhu, Y.; Li, G.; Zhang, S.; Song, J.; Mao, C.; Wu, J.; Jin, B.; Tian, Y. A novel hydrogen peroxide biosensor based on the BPT/AuNPs/graphene/HRP composite. *Sci. China Chem.* **2011**, *54*, 1645–1650. [CrossRef]
34. Sardaremelli, S.; Hasanzadeh, M.; Seidi, F. Enzymatic recognition of hydrogen peroxide (H_2O_2) in human plasma samples using HRP immobilized on the surface of poly(arginine-toluidine blue)-Fe_3O_4 nanoparticles modified polydopamine; A novel biosensor. *J. Mol. Recognit.* **2021**, *34*, e2928. [CrossRef] [PubMed]
35. Dai, H.; Lu, W.; Zuo, X.; Zhu, Q.; Pan, C.; Niu, X.; Liu, J.; Chen, H.; Chen, X. A novel biosensor based on boronic acid functionalized metal-organic frameworks for the determination of hydrogen peroxide released from living cells. *Biosens. Bioelectron.* **2017**, *95*, 131–137. [CrossRef]
36. Cao, L.; Lin, Z.; Peng, F.; Wang, W.; Huang, R.; Wang, C.; Yan, J.; Liang, J.; Zhang, Z.; Zhang, T.; et al. Self-Supporting Metal-Organic Layers as Single-Site Solid Catalysts. *Angew. Chem.-Int. Ed.* **2016**, *55*, 4962–4966. [CrossRef]